Melting of the Wigner lattice at T=0

Lenac, Z.; Šunjić, Marijan

Source / Izvornik: **Physical Review B (Condensed Matter), 1995, 52, 11238 - 11247**

Journal article, Published version
Rad u časopisu, Objavljena verzija rada (izdavačev PDF)

https://doi.org/10.1103/PhysRevB.52.11238

Permanent link / Trajna poveznica: https://urn.nsk.hr/urn:nbn:hr:217:079969

Melting of the Wigner lattice at $T = 0$

Z. Lenac
Pedagogical Faculty, University of Rijeka, 51000 Rijeka, Croatia

M. Šunjić
Department of Physics, University of Zagreb, P.O. Box 162, 41000 Zagreb, Croatia
(Received 19 April 1995; revised manuscript received 21 June 1995)

A two-dimensional electron system is expected to form a Wigner lattice at zero temperature, but at very high electron densities even at $T = 0$ one expects a phase transition from a crystal to a gas phase. For a Wigner lattice on a dielectric layer, a $T = 0$ melting was also predicted at very low electron densities. Here we explain both high- and low-density phase transitions studying the behavior of an external electron added to the periodic potential of a Wigner lattice. The band structure of this electron is calculated within a model of a quasi-two-dimensional lattice. The $T = 0$ melting criterion is derived, comparing the chemical potentials of an additional electron when it joins the lattice or stays delocalized. Good qualitative agreement is found between our results and those obtained from the quantum extension of the Kosterlitz-Thouless melting theory.

I. INTRODUCTION

The two-dimensional (2D) electron system, even in the absence of an external electromagnetic field, shows very peculiar properties in the low-temperature range. At $T = 0$ it is expected to form a Wigner crystal.[1] The melting of this crystal at $T > 0$ is described as driven by the dissociation of dislocation pairs. Such a melting mechanism was first proposed by Kosterlitz and Thouless[2] and further elaborated by Nelson and Halperin[3] and Young.[4] The predictions of the KTNHY theory were experimentally verified[5] and, e.g., even the intermediate liquid-crystal ("hexatic") phase is now well understood.[6]

However, there still remains one open but very fundamental question: which mechanism determines the phase transition of 2D electrons at $T = 0$? The KTNHY theory is a classical one, valid at $T \gg T_F$. Since the Fermi temperature T_F is proportional to the 2D electron concentration n, at $T \to 0$ strictly speaking KTNHY theory is valid only in the $n \to 0$ limit. Therefore this theory cannot explain the expected melting of a Wigner lattice at $T = 0$ at some finite electron density. An *ad hoc* extension to this "quantum regime" was made by Peeters and Platzman,[7] who in the KTNHY melting criterion simply replaced the kinetic energy term kT, valid for $T \gg T_F$, by its quantum-mechanical version.[8] Although this theory has no clear physical justification, it predicts that at $T = 0$ a Wigner crystal melts into a gas phase at both very low and very high electron densities. These critical densities also depend upon the properties of a dielectric layer when 2D electrons are deposited on it.[7,9]

Another possible approach is to calculate the ground-state energy of a 2D electron system in both crystal and gas phases. It can be done accurately in the simplified model of strictly 2D electrons, immersed in the positive background that provides charge neutrality. Both theoretical[10] and numerical[11] evaluations show that at high electron densities the gas phase has lower energy than the crystal phase. Although the calculations were very precise, the Wigner phase transition was predicted with relatively large uncertainty ($r_s = 37 \pm 5$) because both phases have almost the same energy around the $r_s = 40$ value.[11] Here $r_s = 1/\sqrt{\pi n} a_0$ is an average lateral distance between 2D electrons in units of Bohr radius a_0. [In this paper we shall express electron density by the lattice parameter r_0 (Å) rather than by r_s. But for a 2D hexagonal Wigner lattice it is almost the same: $r_s = 0.992\, r_0$ (Å).]

Note that neither of these theoretical approaches explains the mechanism of the Wigner transition. Although it is believed that this "quantum melting" is continuous, as the thermal melting transition, a possible explanation in terms of point defects[12] was not successful mainly because one cannot use the entropy to lower the free energy of a system at $T = 0$. Instead, one has to calculate the change in zero-point vibration energy due to point defects and compare it with the corresponding change in Coulomb energy. Such calculations are very complicated even for the model of strictly 2D electrons because they require extreme numerical accuracy, otherwise they can lead to wrong conclusions.[12]

In this paper we shall try to explain the $T = 0$ melting of a 2D Wigner lattice treating the electrons in a rather realistic model usually referred to as "quasi-2D electrons." This model is appropriate in the experimental setup where electrons are deposited on a dielectric layer (usually liquid helium) with a metallic substrate, which provides charge neutrality.[9] The image force together with an applied pressing field confine electrons close to but not strictly at a dielectric surface so they behave as a monolayer delocalized in the perpendicular direction. In the crystal phase we assume that delocalized electrons form a perfect 2D hexagonal lattice with a lattice parameter r_0. Then we add an external electron that interacts with this lattice and calculate both its coupling to the static lattice and the lowest-order dynamical corrections. Our final aim is to determine the

ground-state energy of this added electron and to compare it with the chemical potential of an electron in a Wigner lattice. This comparison will show whether it is favorable for an N-electron Wigner lattice to accept an added electron and relax as an $(N+1)$-electron lattice, or whether it is more likely that this electron will remain delocalized. The $T=0$ Wigner transition then occurs at the critical density at which an added electron could no longer be trapped and localized by lattice electrons.

The paper is organized as follows. In Sec. II we first briefly analyze the properties of a quasi-2D Wigner lattice and then focus our attention on the problem of an external electron in a (static) potential of this lattice. The physical parameters determining the external electron wave function are discussed in detail and the electron energy band structure is analyzed. In Sec. III we compare the ground-state energy of an external electron with the chemical potential of lattice electrons. This comparison will give us a clear insight into the Wigner phase transition at $T=0$. The conclusions are given in Sec. IV. The dynamical correction to the electron-lattice interaction, i.e., polaron self-energy, is calculated in the Appendix.

II. ELECTRON IN A PERIODIC POTENTIAL OF A WIGNER LATTICE

Our basic system consists of N electrons that form a quasi-2D Wigner lattice configured on a dielectric layer with a dielectric constant ε. All numerical calculations in this paper are performed for liquid helium ($\varepsilon = 1.057$), which represents a standard experimental setup.[5] The thickness of the layer is d and it is placed on a semi-infinite metallic substrate. Now we add an external electron to interact with lattice electrons. The total Hamiltonian becomes

$$H = H_L + H_e + H_{eL} \ . \tag{1}$$

Here H_L is the electron lattice Hamiltonian:[9]

$$H_L = \sum_i K_i + \sum_i V^{\rm im}(z_i) + \frac{1}{2}\sum_i \sum_{j\neq i} W^{ee}(\boldsymbol{\rho}_i - \boldsymbol{\rho}_j;\, z_i, z_j) \tag{2}$$

and K_i, $V^{\rm im}$, and W^{ee} denote kinetic energy, image potential, and electron-electron interaction, respectively, of lattice electrons at sites z_i above the dielectric surface and at lateral distances $\rho_{ij} = |\boldsymbol{\rho}_i - \boldsymbol{\rho}_j|$.

The explicit form of the image potential is

$$V^{\rm im}(z) = -\frac{1}{2}e^2 \int_0^\infty dk\, D(k)\, e^{-2kz} \tag{3}$$

with the dielectric response function:

$$D(k) = \frac{\beta + e^{-2kd}}{1+\beta e^{-2kd}} \ , \quad \beta = \frac{\varepsilon - 1}{\varepsilon + 1} \ .$$

The electron-electron interaction (direct and image terms) is simply represented in the two-dimensional $\mathbf{k}$ space:

$$W^{ee}(\boldsymbol{\rho};\, z, z') = \frac{S}{(2\pi)^2} \int d\mathbf{k}\, W(\mathbf{k};\, z, z')\, e^{i\mathbf{k}\boldsymbol{\rho}} \ ,$$

$$W(\mathbf{k};\, z, z') = \frac{e^2}{S}\frac{2\pi}{k}\left[e^{-k|z-z'|} - D(k)\, e^{-k(z+z')} \right] \ . \tag{4}$$

Here $S = 1/n$ is an average area per electron. We shall need the $\mathbf{k} \to 0$ limit:

$$W(\mathbf{k}=0;\, z, z') = \frac{e^2}{S} 2\pi \left[\left(\frac{1-\beta}{1+\beta} \right) 2d + (z+z') + |z-z'| \right] \ . \tag{5}$$

The Hamiltonian H_e of an external electron at the lateral position $\boldsymbol{\rho}$ and at distance z above the dielectric surface contains electron kinetic energy K, its image potential $V^{\rm im}(z)$, and its interaction $U(\boldsymbol{\rho}, z)$ with lattice electrons in their regular lateral positions $\boldsymbol{\rho}_i^0$:

$$H_e = K + V^{\rm im}(z) + U(\boldsymbol{\rho}, z) \ , \tag{6}$$

$$U(\boldsymbol{\rho}, z) = \sum_i W^{ee}(\boldsymbol{\rho}_i^0 - \boldsymbol{\rho};\, z_i, z) \ . \tag{7}$$

Therefore H_e describes the behavior of an electron in the static potential of a 2D Wigner lattice.

The remaining term in (1) is obviously the interaction of an electron with the dynamical part of the lattice potential:

$$H_{eL} = \sum_i \left[W^{ee}(\boldsymbol{\rho}_i - \boldsymbol{\rho};\, z_i, z) - W^{ee}(\boldsymbol{\rho}_i^0 - \boldsymbol{\rho};\, z_i, z) \right] . \tag{8}$$

A. Lattice Hamiltonian

In order to point out some relations relevant to our further discussion, we shall first briefly analyze the lattice Hamiltonian (2). We have already solved the problem of a delocalized Wigner lattice above a dielectric surface by assuming the separation of the lattice wave function Ψ_L into "lateral" $v_L(\boldsymbol{\rho}_1 \ldots \boldsymbol{\rho}_N)$ and "perpendicular" $u_L(z_1 \ldots z_N)$ components.[13] For the perpendicular component we have taken a Hartree approximation $u_L(z_1 \ldots z_N) = u_1(z_1) \cdots u_N(z_N)$, and the study of the lateral component enables us (in the harmonic approximation) to derive the phonon spectrum of a 2D Wigner lattice.[14,15]

For the ground state of a lattice we have used the perpendicular, one-electron variational wave function:

$$u_\alpha(z) = 2\,\alpha^{3/2}\, z\, e^{-\alpha z} \ , \tag{9}$$

where the variational parameter α determines the perpendicular delocalization of an electron. The lattice

ground-state energy (per one electron) is given in the form[9]

$$E_L = \langle E^{\rm osc}\rangle + \langle E^{\rm im}\rangle + \tfrac{1}{2}\langle W^{ee}\rangle \ . \tag{10}$$

The first term,

$$\langle E^{\rm osc}\rangle = \frac{1}{N}\sum_{\boldsymbol{\kappa}}\sum_{p}\frac{\hbar}{2}\,\omega_{\boldsymbol{\kappa}p} = \sum_{p}\int_{S_B}\frac{d\boldsymbol{\kappa}}{S_B}\,\frac{\hbar}{2}\,\omega_{\boldsymbol{\kappa}p}\ , \tag{11}$$

represents the contribution from the two phonon modes $p = (-,+)$, usually referred to as longitudinal (L) and transverse (T), respectively. Their frequencies $\omega_{\boldsymbol{\kappa}p}$ and their polarization eigenvectors $\boldsymbol{\epsilon}_{\boldsymbol{\kappa}p}$ were already analyzed.[14,15] Here $\boldsymbol{\kappa}$ is the phonon wave vector and S_B is the surface of the first Brillouin zone (BZ). Since the integrand in Eq. (11) is a periodic function of $\boldsymbol{\kappa}$ ($\omega_{\boldsymbol{\kappa}+\mathbf{G},p} = \omega_{\boldsymbol{\kappa},p}$), the integration over the BZ can be performed as a summation over the characteristic points, as explained in Ref. 16. Let us also note that the $p = (-,+)$ modes are well polarized in the (T,L) directions, respectively, only close to the Γ point in the BZ ($\kappa \ll g_0$), while close to the zone boundary the polarization eigenvectors can deviate significantly from the (T,L) directions. Here g_0 is the reciprocal lattice parameter.

The image energy $\langle E^{\rm im}\rangle$ in Eq. (10) gives the contribution from the perpendicular kinetic energy and the image potential of the lattice electron:

$$\langle E^{\rm im}\rangle = \int dz_i\, u_\alpha^*(z_i)\left[-\frac{\hbar^2}{2m}\frac{\partial^2}{\partial z_i^2} + V^{\rm im}(z_i)\right] u_\alpha(z_i)\ . \tag{12}$$

The last term in Eq. (10) is the average electrostatic potential of lattice electrons in their regular lateral sites:

$$\langle W^{ee}\rangle = \sum_{j\neq i}\int dz_j\,|u_\alpha(z_j)|^2 \times \int dz_i\,|u_\alpha(z_i)|^2\, W^{ee}(\boldsymbol{\rho}_i^0 - \boldsymbol{\rho}_j^0;\, z_i, z_j)\ . \tag{13}$$

When we perform the summation over all electrons in the lattice, an essential step that enables us to remove divergencies is to calculate first $\langle W^{ee}\rangle$ without the Fourier $\mathbf{k} = 0$ component (5) and then to add the contribution from this component in its explicit form:[9]

$$\langle W_0\rangle = \int dz\,|u_\alpha(z)|^2\,\overline{W}(\mathbf{k}=0,z)\ , \tag{14}$$

where we have defined for any $\mathbf{k}$:

$$\overline{W}(\mathbf{k},z) = \int dz_i\,|u_\alpha(z_i)|^2\,W(\mathbf{k};\,z_i,z)\ . \tag{15}$$

If we take Eq. (9) for $u_\alpha(z)$, the z-dependent terms of $W(\mathbf{k}=0;\,z_i,z_j)$, Eq. (5), contribute to $\langle W_0\rangle$ as

$$\langle W_0^{\alpha\alpha}\rangle = 2\pi n e^2\,\frac{33}{16}\,\frac{1}{\alpha}\ . \tag{16}$$

The contribution to $\langle W_0\rangle$ from the z-independent term of $W(\mathbf{k}=0;\,z_i,z_j)$ follows immediately because it does not depend upon the particular shape of the (normalized) function $u_\alpha(z)$:

$$\langle W_0^d\rangle = 2\pi n e^2\left(\frac{1-\beta}{1+\beta}\right)2d\ . \tag{17}$$

Let us point out that the variational parameter α can be determined in two different ways. First, according to the Hartree approximation used for the perpendicular wave function of the lattice u_L, we can determine α by varying independently each electron wave function $u_\alpha(z_i)$. This leads to the standard one-particle Hartree equation for an electron in a central field of other electrons (omitting the factor 1/2 in front of the electron-electron interaction $\langle W^{ee}\rangle$). The minimization of this Hamiltonian gives $\alpha = \alpha_H$, which describes best the one-particle properties. One can obtain the ground-state energy in this way,[15] but usually it is not a very good approximation. A better result for the ground-state energy is obtained if one minimizes the total lattice energy $NE_L(\alpha)$ with respect to α. This will give the value $\alpha = \alpha_E$.

In Eq. (10) $\langle E^{\rm osc}\rangle$ is almost independent of α, but $\langle E^{\rm im}\rangle$ and $\langle W^{ee}\rangle$ depend on it. Because in the total energy NE_L the factor 1/2 appears in front of $\langle W^{ee}\rangle$, we expect a difference between α_H and α_E. This difference is not very large (see the inset in Fig. 2), but we shall still take $\alpha = \alpha_H$ in the calculation of the one-particle properties and $\alpha = \alpha_E$ in the calculation of the phonon spectrum and the ground-state energy of the Wigner lattice.

B. External electron

The problem of an external electron in the periodic potential of a lattice is a standard problem of solid state physics, but here instead of an attractive electron-ion interaction we have a repulsive electron-electron interaction $U(\boldsymbol{\rho},z)$ (7). To find the electron energy ϵ_e in such a potential we shall first average $U(\boldsymbol{\rho},z)$ over the perpendicular lattice coordinates with $|u_L(z_1\ldots z_N)|^2$. This will give $\overline{U}(\boldsymbol{\rho},z)$. As a periodic function of $\boldsymbol{\rho}$ it can be expanded in the Fourier series:

$$\overline{U}(\boldsymbol{\rho},z) = \overline{W}(\mathbf{k}=0,z) + \triangle U(\boldsymbol{\rho},z)\ , \tag{18}$$

$$\triangle U(\boldsymbol{\rho},z) = \sum_{\mathbf{G}\neq 0}\overline{W}(\mathbf{G},z)\,e^{i\mathbf{G}\boldsymbol{\rho}}\ . \tag{19}$$

Here $\mathbf{G}$ is the reciprocal lattice vector of a two-dimensional Wigner lattice and $\overline{W}(\mathbf{G},z)$ is defined by Eq. (15).

Now we have to determine the external electron wave function $\Psi_e(\boldsymbol{\rho},z)$, which satisfies the Schrödinger equation determined by the $\{z_i\}$-averaged electron Hamiltonian (6):

$$[\,K + V^{\rm im}(z) + \overline{U}(\boldsymbol{\rho},z)\,]\,\Psi_e(\boldsymbol{\rho},z) = \epsilon_e\,\Psi_e(\boldsymbol{\rho},z)\ . \tag{20}$$

We are interested in the ground-state energy of this

electron. As in the lattice case, we shall write $\Psi_e(\boldsymbol{\rho}, z)$ as a product of the perpendicular $u_e(z)$ and parallel $\psi_e(\boldsymbol{\rho})$ components:

$$\Psi_e(\boldsymbol{\rho}, z) = u_e(z)\,\psi_e(\boldsymbol{\rho}) \ .$$

The form of the image potential $V^{\rm im}(z)$ then suggests to take for $u_e(z)$ the same form as in Eq. (9), with the variational parameter $\alpha = \alpha_e$.

The parallel component $\psi_e(\boldsymbol{\rho})$ should satisfy the Bloch theorem:

$$\psi_e(\boldsymbol{\rho}) = e^{i\boldsymbol{\kappa}\boldsymbol{\rho}}\,\psi_{\boldsymbol{\kappa}}(\boldsymbol{\rho}) \ , \tag{21}$$

where $\boldsymbol{\kappa}$ is the wave vector in the BZ. If we assume that an external electron is localized in between the lattice electrons, we can describe it by Wannier functions $\Phi(\boldsymbol{\rho})$ localized at those sites:

$$\psi_{\boldsymbol{\kappa}}(\boldsymbol{\rho}) = \sum_j e^{-i\boldsymbol{\kappa}(\boldsymbol{\rho}-\boldsymbol{\rho}_j^0)}\,\Phi(\boldsymbol{\rho}-\boldsymbol{\rho}_j^0) \ . \tag{22}$$

In the primitive hexagonal lattice there are two centered interstitial sites: $\mathbf{s}_1 = (\mathbf{a}+\mathbf{b})/3$ and $\mathbf{s}_2 = 2\mathbf{s}_1$ (Fig. 1) where the electrostatic potential energy of an external electron has a minimum. In the vicinity of these points the potential energy is nearly harmonic so we can put

$$\Phi(\boldsymbol{\rho}-\boldsymbol{\rho}_j^0) = \frac{C}{\sqrt{A}}\,\frac{1}{2}\,\left[\phi(\boldsymbol{\rho}-\boldsymbol{\rho}_j^0-\mathbf{s}_1) + \phi(\boldsymbol{\rho}-\boldsymbol{\rho}_j^0-\mathbf{s}_2)\right] \ , \tag{23}$$

$$\phi(\boldsymbol{\rho}) = e^{-\rho^2/2\sigma_e^2} \ .$$

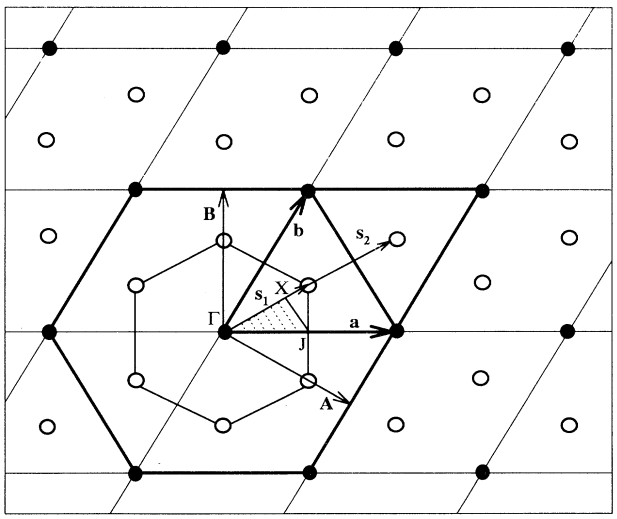

FIG. 1. 2D hexagonal lattice with the primitive vectors $\mathbf{a}, \mathbf{b}$. Full circles represent the regular positions of lattice electrons and empty circles the most probable positions of an external electron. Empty circles form peaks of a hexagon around each lattice electron. We have also shown reciprocal lattice vectors $\mathbf{A}, \mathbf{B}$ and the belonging irreducibile part of the BZ, determined by the special points Γ, X, and J.

Here $A = NS$ is the total area of the lattice, C is the normalization constant, and σ_e is the variational parameter that determines the lateral delocalization of an electron. [Additionally, for the centered interstitial sites $(\mathbf{s}_1, \mathbf{s}_2)$, we have also calculated the electron wave function localized at the edge interstitial sites, i.e., between two lattice electrons, but this wave function gives higher electron energy.[12]]

Let us expand the periodic function $\psi_{\boldsymbol{\kappa}}(\boldsymbol{\rho})$ (22) in the Fourier series:

$$\psi_{\boldsymbol{\kappa}}(\boldsymbol{\rho}) = \frac{C}{\sqrt{A}} \sum_{\mathbf{G}} \eta_{\boldsymbol{\kappa}}(\mathbf{G})\, e^{i\mathbf{G}\boldsymbol{\rho}} \ .$$

Taking the Fourier components of the Gaussian function $\phi(\boldsymbol{\rho})$, we obtain $(\mathbf{k} = \boldsymbol{\kappa} + \mathbf{G})$

$$\eta_{\boldsymbol{\kappa}}(\mathbf{G}) = 2\pi n\sigma_e^2\, e^{-\frac{i}{2}\mathbf{k}(\mathbf{s}_1+\mathbf{s}_2)}\,\cos[\tfrac{1}{2}\mathbf{k}(\mathbf{s}_1-\mathbf{s}_2)]\, e^{-\frac{1}{2}\sigma_e^2 k^2} \ .$$

The coefficient C in Eqs. (23) and (22) follows from the normalization condition for $\psi_e(\boldsymbol{\rho})$:

$$C_{\boldsymbol{\kappa}}^{-2} = \sum_{\mathbf{G}} |\eta_{\boldsymbol{\kappa}}(\mathbf{G})|^2 \ .$$

Now we can integrate the Schrödinger equation (20) to obtain the energy of an external electron interacting with the (static) potential of a Wigner lattice:

$$\epsilon_e = \langle\epsilon^{\rm kin}\rangle + \langle\epsilon^{\rm im}\rangle + \langle\epsilon^{\rm pot}\rangle \ . \tag{24}$$

The parallel kinetic energy of an electron is

$$\langle\epsilon^{\rm kin}\rangle = \frac{1}{2}e^2 a_0 \left[\kappa^2 + C_{\boldsymbol{\kappa}}^2 \sum_{\mathbf{G}\neq 0} (G^2 + 2\boldsymbol{\kappa}\mathbf{G})\,|\eta_{\boldsymbol{\kappa}}(\mathbf{G})|^2\right] \ .$$

The image energy has the same form as in the lattice case (12) but with the variational parameter α_e. It gives

$$\langle\epsilon^{\rm im}\rangle = \frac{1}{2}e^2\left[a_0\alpha_e^2 - \int_0^\infty dk\,\frac{D(k)}{(1+k/\alpha_e)^3}\right] \ .$$

The potential energy derived from the electron-lattice interaction $\overline{U}(\boldsymbol{\rho}, z)$ has three terms, which according to Eqs. (18) and (19) are

$$\langle\epsilon^{\rm pot}\rangle = \langle W_0^d\rangle + \langle W_0^{\alpha_H\alpha_e}\rangle + \langle\triangle U\rangle \ . \tag{25}$$

The first two terms in Eq. (25) are obtained by taking the z average of the $\mathbf{G} = 0$ component $\overline{W}(\mathbf{k} = 0, z)$ of the lattice potential (18). The first term $\langle W_0^d\rangle$ is obtained from the z-independent term of Eq. (5) so we immediately find the previous result (17). The second term $\langle W_0^{\alpha_H\alpha_e}\rangle$ is obtained by averaging the z-dependent terms of Eq. (5) with two different functions $|u_{\alpha_H}|^2$ and $|u_{\alpha_e}|^2$, which describe the perpendicular density of a lattice and an external electron, respectively. It gives

$$\langle W_0^{\alpha_H \alpha_e} \rangle = 2\pi n e^2 \frac{3}{\alpha_H} \left\{ 1 - \alpha_H^3 \left[\frac{1}{(\alpha_H + \alpha_e)^3} + \frac{2\alpha_H}{(\alpha_H + \alpha_e)^4} + \frac{2\alpha_H^2}{(\alpha_H + \alpha_e)^5} \right] \right\} . \quad (26)$$

For $\alpha_e = \alpha_H = \alpha$, Eq. (26) turns into the result (16) for $\langle W_0^{\alpha\alpha} \rangle$.

The third term in Eq. (25) is calculated with the help of the $\mathbf{G}$ expansion of both $\triangle U(\boldsymbol{\rho}, z)$ (19) and $\psi_{\boldsymbol{\kappa}}(\boldsymbol{\rho})$ (22):

$$\langle \triangle U \rangle = C_{\boldsymbol{\kappa}}^2 \sum_{\mathbf{G} \neq 0} \int_0^\infty dz \, |u_{\alpha e}(z)|^2 \, \overline{W}(\mathbf{G}, z) \times \sum_{\mathbf{G}'} \eta_{\boldsymbol{\kappa}}^*(\mathbf{G}') \eta_{\boldsymbol{\kappa}}(\mathbf{G}' - \mathbf{G}) . \quad (27)$$

The variational parameters (α_e, σ_e) can now be obtained by the minimization of $\epsilon_e(\boldsymbol{\kappa})$ in Eq. (24) with respect to these parameters. To obtain the total ground-state energy of an external electron we have to add to ϵ_e also the contribution ϵ_{eL} from the dynamical part of electron-lattice interaction, which is described by the Hamiltonian (8). This contribution is calculated in the Appendix.

C. Discussion of an external electron wave function and of $\epsilon_e(\boldsymbol{\kappa})$ dependence

The wave function $\Psi_e(\boldsymbol{\rho}, z)$ of an external electron is determined, for a given $\boldsymbol{\kappa}$, by two parameters: α_e and σ_e. We shall first analyze their ground-state ($\boldsymbol{\kappa} = 0$) values.

The "perpendicular" parameter α defines the average position $\langle z \rangle = 3/2\alpha$ of an electron above a dielectric surface. For an external electron, Fig. 2 shows that $\langle z_e \rangle$ increases with increasing r_0 similarly as does $\langle z_H \rangle$ in the case of lattice electrons.[13] At high electron densities ($r_0 \lesssim 100$ Å) the direct electron-electron interaction is very strong and the thickness of a dielectric layer has almost no influence on $\langle z_e \rangle$.[9] But at lower electron densities, the image potential becomes more important, particularly in the case of thin dielectric layers ($d \lesssim 100$ Å) where it clearly reduces $\langle z_e \rangle$ values.

In the inset of Fig. 2 we have compared $\langle z_e \rangle$ and $\langle z_H \rangle$. At higher electron densities ($r_0 \lesssim 1000$ Å), an external electron is efficiently repelled by lattice electrons so we find $\langle z_e \rangle > \langle z_H \rangle$. At $r_0 \gtrsim 1000$ Å, the electron repulsion is very weak and both $\langle z_e \rangle$ and $\langle z_H \rangle$ are mainly determined by the same image potential, which gives $\langle z_e \rangle \approx \langle z_H \rangle$.

The lateral spread of an external electron wave function is determined by the parameter σ_e. Figure 3 shows the ratio σ_e/r_0. At thin dielectric layers ($d \lesssim 100$ Å) and at low electron densities ($r_0 \gtrsim 1000$ Å) the well-screened lattice electrons weakly interact with an external electron, which leads to a large spread of an external electron wave function.

In our model, lattice electrons are described in a harmonic approximation as phonons. As a simple test of this approximation we can define the lateral spread of lattice electrons $\langle \sigma_L \rangle$ through the relation that is satisfied by a 2D harmonic oscillator in the ground state:

$$\langle \sigma_L \rangle = \left(\frac{\hbar}{m \langle \omega \rangle} \right)^{\frac{1}{2}} .$$

Here $\langle \omega \rangle$ is defined as the phonon frequency averaged over

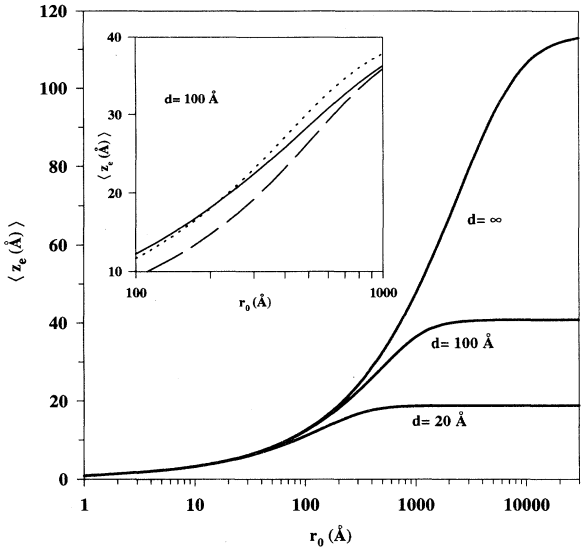

FIG. 2. Average distance $\langle z_e \rangle$ of an external electron above a dielectric surface as a function of r_0, for three different thicknesses d. Inset: The comparison between $\langle z_e \rangle = 3/2\alpha_e$ (full line) and $\langle z_H \rangle = 3/2\alpha_H$ (dashed line) values. We also give $\langle z_E \rangle = 3/2\alpha_E$ curve (dotted line) in order to show the difference between α_H and α_E.

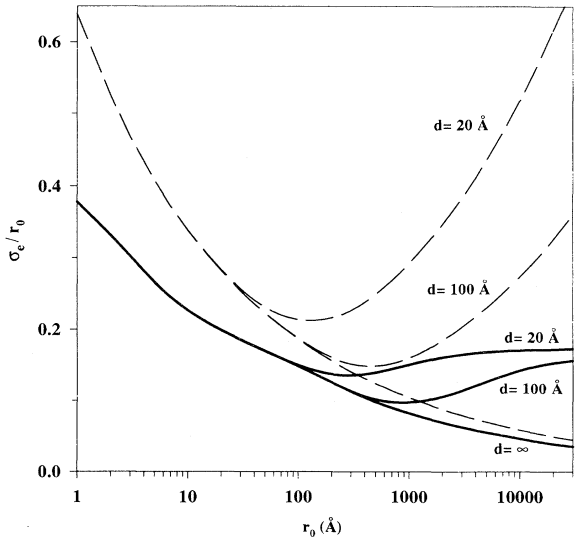

FIG. 3. Relative spread σ_e/r_0 of an external electron wave function as a function of r_0, for three different thicknesses d and for $\boldsymbol{\kappa} = 0$. Dashed lines represent corresponding values σ_L/r_0 for lattice electrons, calculated from the phonon model.

the two phonon modes and over the BZ, as in Eq. (11). The ratio σ_L/r_0 is also shown in Fig. 3. Suprisingly, it gives a resonable result even in the very high density limit.

Let us point out some limitations of our theory.

(i) The true Wannier functions are defined as orthogonal for different lattice points, but our choice (23) will strictly satisfy this condition only in the $\sigma_e \to 0$ limit. For other σ_e values, Wannier functions (23) will depend upon $\boldsymbol{\kappa}$ and therefore we have to minimize $\epsilon_e(\boldsymbol{\kappa})$ in Eq. (24) for each $\boldsymbol{\kappa}$. As a result, both variational parameters (α_e, σ_e) depend upon $\boldsymbol{\kappa}$. This dependence should be negligible for *small* σ_e ($\sigma_e \lesssim r_0/4$), because in that case Wannier functions (23) are well localized and therefore almost orthogonal, mostly at lower electron densities. At that limit our theory simply represents the tight-binding approximation. At higher electron densities the overlap between Wannier functions (23) at different primitive cells is not negligible so we expect that (α_e, σ_e) in that case will depend upon $\boldsymbol{\kappa}$ stronger. Finally, in the limit of *large* σ_e, an external electron becomes delocalized. But then we notice that in all energy terms that include summation over $\mathbf{G}$, the convergence is achieved through the terms $\exp(-\sigma_e^2 G^2)$. We can neglect their contributions for $\sigma_e g_0 \gtrsim 3$, so the relation $1/g_0 = (\sqrt{3}/4\pi) r_0 \approx 0.14 r_0$ enables us to take the $\sigma_e \to \infty$ limit for $\sigma_e \gtrsim r_0/2$. In that case only $\mathbf{G} = 0$ terms remain and we immediately obtain the electron energy ϵ_e as if an electron were described by a plane wave $\exp(i\boldsymbol{\kappa}\boldsymbol{\rho})$. In that sense $\psi_e(\boldsymbol{\rho})$ will give a correct physical description of an external electron for all σ_e values, which could be essential when one minimizes an electron energy with respect to σ_e.

(ii) Although the external electron wave function is defined for all σ_e values, we have not orthogonalized it to the lattice electron wave function and included the exchange processes of an external electron with lattice electrons. The first requirement would raise and the second process would lower the energy of an external electron. Both those contributions are negligible if the overlap between the external and the lattice electron wave functions is negligible. This happens for $\sigma_L/r_0 \lesssim 1/4$ and $\sigma_e/r_0 \lesssim 1/4$, i.e., for $r_0 \gtrsim 20$ Å. At higher electron densities our theory is not expected to be very accurate.

(iii) We have not taken into account the influence ot the pressing field $\mathcal{E}$, which is normally applied in the z direction in order to press the 2D electrons on the dielectric surface. Its contribution $\langle E^{\rm pr} \rangle$ to the energy of lattice electrons (10) and $\langle \epsilon^{\rm pr} \rangle$ to the energy of an external electron (24) can be easily calculated:

$$\langle E^{\rm pr} \rangle = e\mathcal{E}\langle z_H \rangle \ , \ \langle \epsilon^{\rm pr} \rangle = e\mathcal{E}\langle z_e \rangle \ .$$

At high electron densities these two contributions differ because of the difference between the $\langle z_H \rangle$ and $\langle z_e \rangle$ values, but for standard macroscopic fields ($\mathcal{E} \lesssim 500$ V/cm)[5], both contributions are negligible in comparison with the strong Coulomb interaction. At low electron densities and for large pressing fields, the terms $\langle E^{\rm pr} \rangle$ and $\langle \epsilon^{\rm pr} \rangle$ can noticeably contribute to the electron energies E_L and ϵ_e, respectively. But in that case we find $\langle z_H \rangle \approx \langle z_e \rangle$, so these two contributions are practically the same and almost independent of electron density. In that sense the pressing field will not change the difference between the crystal and the external electron chemical potential, which will be intensively discussed in Sec. III.

Now we shall analyze the influence of $\boldsymbol{\kappa}$ on variational parameters. As expected, the "perpendicular" parameter α_e turns out to be almost independent of $\boldsymbol{\kappa}$, so in Fig. 4 we show only $\sigma_e(\boldsymbol{\kappa})$. Notice that at high electron densities ($r_0 \lesssim 15$ Å), $\sigma_e(\kappa \approx g_0/2)$ can take much higher values than $\sigma_e(\kappa = 0)$. But at $r_0 = 30$ Å and particularly at lower electron densities σ_e becomes almost independent of $\boldsymbol{\kappa}$. The periodicity requirement $\sigma_e(\boldsymbol{\kappa}) = \sigma_e(\boldsymbol{\kappa}+\mathbf{G})$ can be clearly seen around the X point, because this point exactly divides the $\mathbf{G} = \mathbf{A} + \mathbf{B}$ reciprocal lattice vector (Fig. 1).

The parameters $\sigma_e(\boldsymbol{\kappa})$ and $\alpha_e(\boldsymbol{\kappa})$ are derived from the minimization of electron energy $\epsilon_e(\boldsymbol{\kappa})$. The energy difference $\triangle\epsilon_e(\boldsymbol{\kappa}) = \epsilon_e(\boldsymbol{\kappa}) - \epsilon_e(\boldsymbol{\kappa} = 0)$ is shown in Fig. 5. Notice that at high electron densities ($r_0 \lesssim 30$ Å) and at small wave vectors ($\kappa/g_0 \ll 1$) the effective mass of an external electron $m^* = \hbar^2(\partial^2\epsilon_e/\partial\boldsymbol{\kappa}^2)^{-1}$ is even smaller than the free-electron mass m. At the BZ boundary ($\kappa/g_0 \approx 0.5$), the large σ_e/r_0 values (Fig. 4) suggest that one can take only a few $\mathbf{G}$ components in Eq. (22) to construct the electron wave function. As a test we have taken three suitably chosen $\mathbf{G}$ components and treating the corresponding coefficients $\eta_\kappa(\mathbf{G})$ as variational parameters, we have obtained practically the same $\epsilon_e(\boldsymbol{\kappa})$ values as in Fig. 5.

At lower electron densities the bandwidth becomes much smaller, as it is closely related to the overlap of

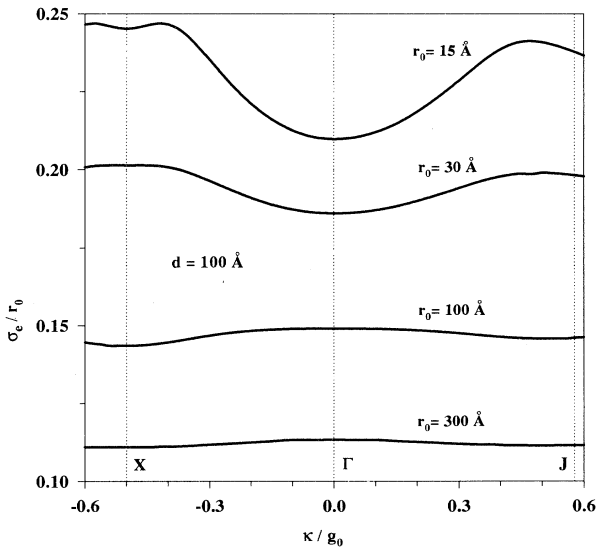

FIG. 4. Relative spread σ_e/r_0 of an external electron wave function as a function of $\boldsymbol{\kappa}$, for various r_0 values. We took $\boldsymbol{\kappa}$ (in units of the reciprocal lattice parameter g_0) along the two characteristic directions of the BZ. The thickness of a dielectric layer is $d = 100$ Å, but similar curves are obtained for other d values.

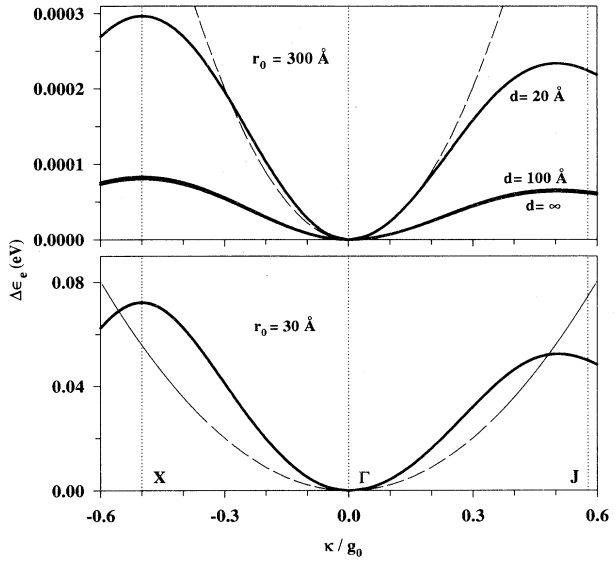

FIG. 5. Energy of an external electron $\triangle\epsilon_e$ as a function of $\boldsymbol{\kappa}$ taken along the ΓX and ΓJ direction of the BZ. At r_0 = 300 Å three different $\triangle\epsilon_e(\boldsymbol{\kappa})$ curves are obtained for three different d values. At r_0 = 30 Å all three d values give the same $\triangle\epsilon_e(\boldsymbol{\kappa})$ curve. Dashed lines represent the free-electron curves $\epsilon_0(\boldsymbol{\kappa}) = \hbar^2\kappa^2/2m$.

the external electron wave function centered at different lattice sites, i.e., to the σ_e/r_0 ratio. Therefore the electron effective mass becomes large ($m^* \gg m$), particularly if electrons are not well screened ($d \gtrsim 100$ Å). But for d = 20 Å strong image potential screens the repulsive electron-electron interaction and an external electron for small $\boldsymbol{\kappa}$ travels in the $\boldsymbol{\rho}$ direction almost freely.

III. WIGNER TRANSITION AT $T = 0$

As pointed out in the Introduction, the main result that we wish to obtain in this paper is to determine electron densities at which a 2D Wigner crystal melts at $T = 0$ into a 2D electron gas. In that sense we shall first define $\triangle E$ as the energy difference between the $(N+1)$-particle Wigner lattice and the N-particle Wigner lattice interacting with an external electron. We can write $\triangle E$ as

$$\triangle E = \mu_L - \mu_e \ , \tag{28}$$

where μ_L is the chemical potential of a Wigner lattice:

$$\mu_L = (N+1)\,E_L(N+1) - N\,E_L(N) = \frac{\partial}{\partial n}\,[nE_L(n)]$$

and μ_e can be regarded as the chemical potential of an external electron. It is its ground-state energy that contains both the static and the dynamical contribution from the electron-lattice interaction:

$$\mu_e = \epsilon_e(\boldsymbol{\kappa} = 0) + \epsilon_{eL} \ .$$

The main contribution to both μ_L and μ_e comes from the term $\langle W_0^d \rangle$ (17) which even diverges for $d \to \infty$. This term has a factor 1/2 in Eq. (10) for E_L, but because of $\langle W_0^d \rangle \sim n$ we find that both μ_L and μ_e contain $\langle W_0^d \rangle$ with the same factor 1 in front. Therefore this term is simply canceled in Eq. (28) for $\triangle E$ and we can define "shifted" chemical potentials as

$$\mu_L' = \mu_L - \langle W_0^d \rangle = \frac{\partial}{\partial n}\,[nE_L'(n)] \ ,$$

$$\mu_e' = \mu_e - \langle W_0^d \rangle = \epsilon_e'(\boldsymbol{\kappa} = 0) + \epsilon_{eL} \ ,$$

where E_L' and ϵ_e' are defined by Eqs. (10) and (24), respectively, but without the $\langle W_0^d \rangle$ term. Now we can easily calculate and compare μ_L' and μ_e' terms since they remain finite for any dielectric thickness d. If we obtain for a particular (n, d) value that $\mu_L' < \mu_e'$, i.e., $\triangle E < 0$, the $(N+1)$-particle system will be a Wigner lattice. However, for $\mu_L' > \mu_e'$, we find $\triangle E > 0$, and the $(N+1)$-particle system will consist of an N-particle Wigner lattice and an external electron that interacts with it. Thus $\triangle E = 0$ can be regarded as the sign of the Wigner phase transition.

The renormalized chemical potentials μ_L' and μ_e' are shown in Fig. 6, where we have also shown the renormalized energy of a lattice electron E_L'. At high electron densities, Fig. 6(a), E_L' is significantly lower than μ_L' as a consequence of a large gradient of a function $E_L'(r_0)$, for $r_0 \lesssim 50$ Å. The function $E_L'(r_0)$ has a minimum around $r_0 \approx 70$ Å and it tends rather smoothly to zero at smaller electron densities, Fig. 6(b). Therefore we find $E_L' > \mu_L'$ at that density region.

At high electron densities, Fig. 6(a), E_L' and μ_L' are practically independent of d, and for each d value we can determine the points at which $\mu_L' = \mu_e'$. It happens at critical lattice parameters $r_c \approx 36$ Å for $d \to \infty$, $r_c \approx 60$ Å for d = 100 Å and there is no crossing for d = 20 Å. If one neglects other effects that can destroy the lattice[19] (electron tunneling, surface roughness, etc.), one can interpret this result as follows.

Let us add, at $r_0 > r_c$, an external electron to a Wigner lattice of N electrons. At first it will most probably come to a position denoted by empty circles in Fig. 1. In the interaction with lattice electrons it can move within the lattice and push the lattice electrons to new positions, as e.g., in the simplified case of a Landau polaron.[20] Finally, we assume, the lattice will relax as an $(N+1)$-electron Wigner lattice. This mechanism works until one reaches the critical density, with $r_0 = r_c$. If one now adds one more electron, it will strongly interact with lattice electrons and its wave function will rather be delocalized: an added electron will travel along the lattice rather than become a lattice electron. Interacting with lattice electrons, it will act as a "trigger" mechanism to destroy the lattice, so the lattice will melt into an electron gas. This added electron, which in fact can be regarded as any of the displaced lattice electrons, now plays a role of a dissociated dislocation pair, which destabilizes the lattice at $T > 0, r_0 \gg r_c$.

At lower electron densities, Fig. 6(b), there is no clear crossover between the μ'_L and μ'_e curves. In fact, at the $d \to \infty$ limit we find $\mu'_L < \mu'_e$ even at $r_0 \to \infty$, i.e., the Wigner lattice remains stable even at very low electron densities. At low electron densities, but at finite d values, the electrons with their images form a dipole layer that tends to distroy the Wigner lattice. Namely, for $d = 100$ Å we find almost the same values for μ'_L and μ'_e at $r_0 \gtrsim 400$ Å. They are determined mainly by the same image potential because the perpendicular parameters α_e and α_H are now almost equal. In these circumstances one electron out of $N+1$ electrons in a Wigner lattice can take place, e.g., in between the regular lattice points with equal probability. Even if the lattice would relax, it would end up with N electrons, i.e., with lower concentration, so the same proces can be continued. Finally, we shall find randomly distributed electrons, which we recognize as an electron gas that interacts with the substrate. At $d = 20$ Å the image potential is so strong that it prevents formation of a Wigner lattice at any electron density.

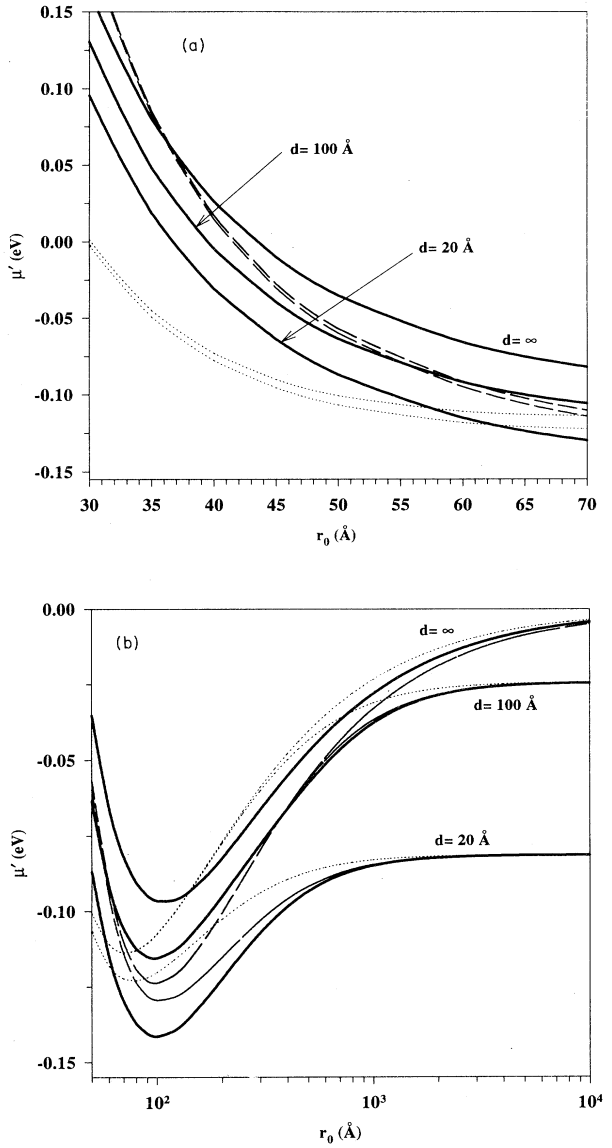

FIG. 6. Renormalized chemical potential of an external electron μ'_e (full lines) and of a Wigner lattice μ'_L (dashed lines) as a function of r_0. Dotted lines represent the renormalized energy (per electron) E'_L of a Wigner lattice. The scale for r_0 is (a) linear in the high-density region, and (b) logarithmic in the low-density region. Notice that in (a) the $\mu'_L(r_0)$ curves are the same for $d = 100$ Å and $d = \infty$ and are both above the corresponding $d = 20$ Å curve. The same holds for $E'_L(r_0)$ curves.

IV. CONCLUSION

Using simple physical arguments, we have been able to explain the melting of a quasi-2D Wigner lattice at $T = 0$. The lattice electrons were described by the phonon model and their interaction with the external electron was calculated using the standard many-body techniques. We have derived the chemical potential of an electron in the Wigner lattice as well as the ground-state energy of the external electron. By comparing them we have determined the critical lattice parameters r_c, which give the critical electron densities at which the Wigner phase transition occurs.

We have mentioned in the Introduction that the rigorous numerical ground-state calculations of Ref. 11, performed for perfectly flat 2D electrons, determined r_c within a relatively large error of 20%, because the crystal and gas phases have almost the same energies around the critical density. Similarly, we have obtained close values for chemical potentials of a lattice electron and of an external electron around the critical lattice parameters (Fig. 6). Although we were not able to determine precisely all possible errors introduced by our approximations, we can expect roughly the same uncertainty in our r_c values. Apart from this, we have shown explicitly the following.

(i) At *high electron densities* the $T = 0$ phase transition occurs when the Wigner lattice becomes "overcharged" in the sense that due to strong Coulomb repulsion a liquid state of an added electron becomes energetically more favorable than its crystal state. An important term that determines r_c values at those densities is the electron-phonon interaction i.e., polaron self-energy. Performing a calculation without this term, one would obtain a phase transition at much higher electron densities.

(ii) At *low electron densities* the behavior of the 2D electron system is determined mainly by the image potential. For infinitely thick dielectric layers this potential is very weak so the electron-electron interaction forms a lattice that will not melt into an electron gas. At finite dielectric thicknesses the image potential, caused mainly by a metallic substrate below the dielectric layer, will screen the electron-electron interaction and even a weak perturbation can lead to the melting of a Wigner lattice.

As pointed out in the Introduction, the *ad hoc* quantum-mechanical extension of KTHNY theory gen-

erally predicts two r_c values.[7–9] For $d \to \infty$, at high electron densities one finds $r_c \approx 60$ Å and at low densities $r_c \to \infty$.[9] We have obtained the same low-density result, but at high densities our result $r_c \approx 36$ Å is closer to the Tanatar-Ceperley result[11] $r_c \approx 37$ Å, derived for perfectly flat 2D electrons.

For $d = 100$ Å the "extended" KTHNY theory gives $r_c \approx 70$ Å in the high- and $r_c \approx 3000$ Å in the low-density region,[9] but in the latter region the transition temperature becomes very small. For $r_0 \gtrsim 700$ Å it falls below 1 K, so it is obviously difficult to determine the exact r_c value for the $T = 0$ transition. We have obtained $r_c \approx 60$ Å in the high-density region and our calculations were not precise enough to determine unambiguously the low-density r_c value, which is roughly estimated to be $r_c \gtrsim 400$ Å.

For $d = 20$ Å both our and "extended" KTHNY theories lead to the same conclusion: strong image potential prevents the formation of a Wigner lattice. Having in mind that the "extended" KTHNY theory is essentially given as a simple balance between the electron kinetic and potential energies, the agreement between this and our theory is quite satisfactory.

APPENDIX: POLARON SELF-ENERGY

In Sec. II we have calculated the interaction of an external electron with the static potential of a Wigner lattice. Here we shall calculate the dynamical correction, i.e., the electron-phonon interaction. This energy correction, usually called the polaron self-energy, is expected to be more important for the Wigner lattice than for a standard atomic lattice, because the electrons that form a Wigner lattice are much lighter than atoms.

The electron-phonon interaction H_{eL} (8) takes in $\mathbf{k}$ space the standard form[17]

$$H_{eL} = \frac{1}{N} \sum_{\mathbf{k}} \sum_{j=1}^{N} W^{ee}(\mathbf{k}; z_j, z)\, e^{i\mathbf{k}\boldsymbol{\rho}} e^{-i\mathbf{k}\boldsymbol{\rho}_j^0} \left(e^{-i\mathbf{k}\mathbf{u}_j} - 1\right) , \tag{A1}$$

where $\mathbf{u}_j = \boldsymbol{\rho}_j - \boldsymbol{\rho}_j^0$ is a displacement of a lattice electron j from its equilibrium position.

The usual approximation is to expand the $\exp(-i\mathbf{k}\mathbf{u}_j)$ term in H_{eL} around $\mathbf{u}_j = 0$ and to keep only the linear term in $\mathbf{u}_j$. In that case only the $0 \to 1$ phonon processes are possible. This approximation is obviously correct for small electron displacements, i.e., for small σ_L/r_0 values and we have already accepted this condition.

After H_{eL} is averaged over perpendicular lattice coordinates with the function $|u_L(z_1 \dots z_N)|^2$, we find[17]

$$\overline{H}_{eL} = \sum_{\mathbf{k}} \sum_{p} e^{i\mathbf{k}\boldsymbol{\rho}}\, M_{\mathbf{k}p}\, (a_{\boldsymbol{\kappa}p} + a^{\dagger}_{-\boldsymbol{\kappa}p}) ,$$

where $a_{\boldsymbol{\kappa}p}$ are standard boson operators and

$$M_{\mathbf{k}p} = \frac{1}{\sqrt{N}}\, \overline{W}(\mathbf{k}, z) \left(\frac{\hbar}{2m\omega_{\boldsymbol{\kappa}p}}\right)^{\frac{1}{2}} k \cos\Phi_p(\mathbf{k}, \boldsymbol{\kappa}) .$$

The summation extends over all $\mathbf{k} = \boldsymbol{\kappa} + \mathbf{G}$ values. Usually only the $\mathbf{G} = 0$ term is calculated. However, we have pointed out that we have to take into account all $\mathbf{G}$ terms for which $\sigma_e G \lesssim 3$.

The polarization angle Φ_p is defined for any wave vector $\mathbf{k} = \boldsymbol{\kappa} + \mathbf{G}$ as

$$\cos\Phi_p(\mathbf{k}, \boldsymbol{\kappa}) = \frac{\mathbf{k}}{k} \cdot \boldsymbol{\epsilon}_{\boldsymbol{\kappa}p} .$$

The polaron self-energy can be calculated with various many-body techniques and probably the best results are obtained as the second-order term in the Schrödinger-Rayleigh perturbation expansion:[17]

$$\epsilon_{eL} = -\sum_{p} \sum_{\boldsymbol{\kappa}} \frac{1}{\triangle\epsilon(\boldsymbol{\kappa}p)} \left| \sum_{\mathbf{G}} \langle \boldsymbol{\kappa}e | M_{\mathbf{k}p}(z)\, e^{i\mathbf{k}\boldsymbol{\rho}} | 0e \rangle \right|^2 . \tag{A2}$$

Here $|\boldsymbol{\kappa}e\rangle$ denotes the external electron wave function. The energy difference between an excited one-phonon state $|1f\rangle|\boldsymbol{\kappa}e\rangle$ and the ground-state $|0f\rangle|0e\rangle$ of the electron-phonon system is

$$\triangle\epsilon(\boldsymbol{\kappa}p) = \hbar\omega_{\boldsymbol{\kappa}p} + \epsilon_e(\boldsymbol{\kappa}) - \epsilon_e(0) . \tag{A3}$$

Notice that we have not included the summation over electron excitations in higher (perpendicular) electron bands. These excitations involve high electron energies[18] and we have estimated their contribution to ϵ_{eL} to be negligible.

After some manipulation, Eq. (A2) can be put in the form

$$\epsilon_{eL} = -\frac{1}{2} e^2 a_0\, n^2 a_0^4 \sum_{p} \int_{S_B} \frac{d\boldsymbol{\kappa}}{S_B} \frac{f_p(\boldsymbol{\kappa})}{\omega_{\boldsymbol{\kappa}p}\, \triangle\epsilon(\boldsymbol{\kappa}p)} , \tag{A4}$$

$$f_p(\boldsymbol{\kappa}) = |C_{\boldsymbol{\kappa}}|^2 |C_0|^2 \left| \sum_{\mathbf{G}} |\boldsymbol{\kappa} + \mathbf{G}| \cos\Phi_p(\boldsymbol{\kappa} + \mathbf{G}, \boldsymbol{\kappa})\, S_{\boldsymbol{\kappa}}(\mathbf{G}) \right|^2 , \tag{A5}$$

$$S_{\boldsymbol{\kappa}}(\mathbf{G}) = \int_0^{\infty} dz\, u^*_{\alpha e\,(\boldsymbol{\kappa})}(z)\, u_{\alpha e\,(0)}(z)\, \overline{W}(\boldsymbol{\kappa} + \mathbf{G}, z) \sum_{\mathbf{G}'} \eta^*_{\boldsymbol{\kappa}}(\mathbf{G}')\, \eta_0(\mathbf{G}' - \mathbf{G}) .$$

In the limit $\sigma_e(\boldsymbol{\kappa}) \to \infty$ only $\mathbf{G} = 0$ terms remain and we obtain a "perpendicularly delocalized" Fröhlich polaron,[17] where

$$f_p(\boldsymbol{\kappa}) = \left| \boldsymbol{\kappa} \cos \Phi_p(\boldsymbol{\kappa}, \boldsymbol{\kappa}) \int_0^\infty dz\, u^*_{\alpha e\,(\boldsymbol{\kappa})}(z)\, u_{\alpha e\,(0)}(z)\, \overline{W}(\boldsymbol{\kappa}, z) \right|^2 .$$

The Bloch energy of an external electron is a periodic function of $\boldsymbol{\kappa}$: $\epsilon_e(\boldsymbol{\kappa}) = \epsilon_e(\boldsymbol{\kappa} + \mathbf{G})$ and so is the function (A5): $f_p(\boldsymbol{\kappa}) = f_p(\boldsymbol{\kappa} + \mathbf{G})$. It means that we can again use the method of Ref. 16 to perform the integration over $\boldsymbol{\kappa}$. As expected, this energy contribution becomes very important at higher electron densities ($r_0 \lesssim 100$ Å) and it greatly reduces the effect of electron repulsion, which is mainly described by the $\mathbf{k} = 0$ terms in Eq. (25).

In this paper we are interested in the external electron ground-state energy, so we have calculated polaron self-energy ϵ_{eL} only for zero electron momentum $\mathbf{p}_e = 0$. The polaron self-energy, calculated for $p_e > 0$ values, could change, e.g., effective electron mass m^*. But to find ϵ_{eL} for $p_e > 0$ is obviously a tedious task. For instance, the energy difference $\triangle\epsilon(\boldsymbol{\kappa}p)$, which appears in the denominator of Eq. (A4) is no longer a periodic function of $\boldsymbol{\kappa}$ and one cannot replace the integration over $\boldsymbol{\kappa}$ with the summation over the characteristic points.[16]

[1] E.P. Wigner, Phys. Rev. **46**, 1002 (1934).
[2] J.M. Kosterlitz and D.J. Thouless, J. Phys. C **6**, 1181 (1973).
[3] D.R. Nelson and B.I. Halperin, Phys. Rev. B **19**, 2457 (1979).
[4] P. Young, Phys. Rev. B **19**, 1855 (1979).
[5] C.C. Grimes and G. Adams, Phys. Rev. Lett. **42**, 795 (1979); D.C. Glatti, E.Y. Andrei, and F.I.B. Williams, *ibid.* **60**, 420 (1988); M.A. Stan and A.J. Dahm, Phys. Rev. B **40**, 8995 (1989).
[6] L.R. Peterson and V.M. Kaganer, Phys. Rev. Lett. **73**, 102 (1994).
[7] F.M. Peeters and P.M. Platzman, Phys. Rev. Lett. **50**, 2021 (1983); F.M. Peeters, Phys. Rev. B **30**, 159 (1984).
[8] P.M. Platzman and H. Fukuyama, Phys. Rev. B **10**, 3150 (1974).
[9] Z. Lenac and M. Šunjić, Phys. Rev. B **46**, 7821 (1992).
[10] M. Jonson, J. Phys. C **9**, 3055 (1976); D.L. Freeman, *ibid.* **16**, 711 (1983); Y. Takada, Phys. Rev. B **30**, 3882 (1984); S. Nagano, K.S. Singwi, and S. Ohniski, *ibid.* **29**, 1209 (1984); Z. Lenac and M. Šunjić, *ibid.* **50**, 10 792 (1994).
[11] B. Tanatar and D.M. Ceperley, Phys. Rev. B **39**, 5005 (1989).
[12] E. Cockayne and V. Elser, Phys. Rev. B **43**, 623 (1991); D.S. Fisher, B.I. Halperin, and R. Morf, *ibid.* **20**, 4692 (1979).
[13] Z. Lenac and M. Šunjić, Phys. Rev. B **43**, 6049 (1991).
[14] L. Bonsall and A.A. Maradudin, Phys. Rev. B **15**, 1959 (1977).
[15] Z. Lenac and M. Šunjić, Phys. Rev. B **44**, 11 465 (1991).
[16] S.L. Cunningham, Phys. Rev. B **10**, 4988 (1974).
[17] See, e.g., G.D. Mahan, *Many Particle Physics*, 3rd ed. (Plenum, New York, 1986).
[18] Z. Lenac and M. Šunjić, Phys. Rev. B **48**, 14 496 (1993).
[19] H. Ikezi and P.M. Platzman, Phys. Rev. B **23**, 1145 (1981); X.L. Hu and A.J. Dahm, *ibid.* **42**, 2010 (1990).
[20] L.D. Landau and S.I. Pekar, Zh. Eksp. Teor. Fiz. **16**, 341 (1946).